ACS APPLIED MATERIALS & INTERFACES

Letter

www.acsami.org

Origin and Electronic Features of Reactive Oxygen Species at Hybrid Zirconia-Acetylacetonate Interfaces

Ana B. Muñoz-García,[†] Filomena Sannino,[‡] Giuseppe Vitiello,[§] Domenico Pirozzi,[§] Luciana Minieri,[§] Antonio Aronne,[§] Pasquale Pernice,[§] Michele Pavone,*[,†] and Gerardino D'Errico*[,†]

[†]Dipartimento di Scienze Chimiche, [‡]Dipartimento di Agraria and [§]Dipartimento di Ingegneria Chimica, dei Materiali e della Produzione Industriale, Università degli Studi di Napoli "Federico II", Napoli, Italia

Supporting Information

ABSTRACT: The hybrid sol–gel zirconia–acetylacetonate amorphous material (HSGZ) shows high catalytic activity in oxidative degradation reactions without light or thermal pretreatment. This peculiar HSGZ ability derives from the generation of highly reactive oxygen radical species (ROS) upon exposure to air at room conditions. We disclose the origin of such unique feature by combining EPR and DRUV measurements with first-principles calculations. The organic ligand acetylacetonate (acac) plays a pivotal role in generating and stabilizing the superoxide radical species at the HSGZ-air interfaces. Our results lead the path toward further development of HSGZ and related hybrid materials for ROS-based energy and environmental applications.

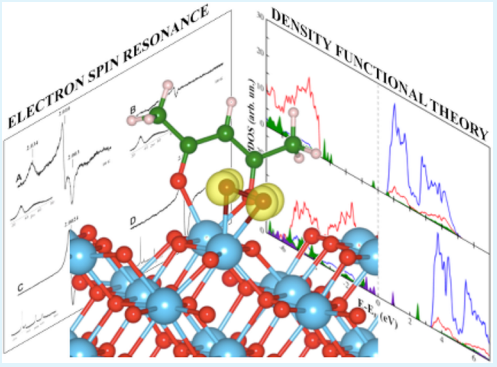

KEYWORDS: *hybrid organic–inorganic material, zirconia, acetylacetonate complex, ROS, EPR, DFT*

Doped and defective transition-metal oxides catalyze the oxidative removal of pollutants in air, water and soil. The prototypical mechanism involves catalyst photoexcitation and subsequent formation of reactive oxygen species (ROS) that act as oxidant agents.[1] However, the most used materials (e.g., TiO_2 and V_2O_5) are only effective under ultraviolet light irradiation, which leads to low quantum efficiencies under sunlight. Doping and defect engineering are the common design strategies toward oxide-based materials with a reduced band gap. Zirconia, for example, with a quite large band gap (~5 eV) has been rarely applied in photocatalysis, but recent works on doped ZrO_2 have reported a promising photosensitivity in the visible region.[2,3] An alternative approach consists of adsorbing suitable ligands or organic molecules on the transition metal oxide surfaces, so to obtain hybrid interfaces with purposely tailored optical and chemical properties.[4]

Some of us have recently applied a sol–gel route to obtain a hybrid ZrO_2 acetylacetonate (acac) material (HSGZ), which presents high remediation activity toward various organic pollutants.[5,6] Contrary to surface modification methods, this technique allowed us to obtain highly homogeneous porous materials in which the functionalities are extended to whole bulk material at the atomic scale. Unexpectedly, HSGZ is catalytically active at room temperature and without any light irradiation.[6] The acac-ZrO_2 interface is key to promoting the formation of the catalytically active ROS, which promote the degradation of organic pollutants (e.g., phenanthrene) through the formation of intermediate free radicals.[5] In this Letter, we investigate the origin and the electronic features leading to the ROS formation by a combined spectroscopic and theoretical approach.

HSGZ samples consist of amorphous polymeric networks of solid zirconia nanoclusters with surface Zr species involved in strong complexation with the acac ligands. The presence of paramagnetic centers at HSGZ surfaces was checked by electron paramagnetic resonance (EPR) measurements, the spectra are shown in Figure 1. The as-dried HSGZ and the reference sol–gel derived zirconia without acac (SGZ) are both amorphous solids as ascertained by X-ray diffraction (XRD, insets in Figure 1A, B).

The HSGZ EPR spectrum, reported in Figure 1A, shows the orthorhombic signal of $O_2^{\bullet-}$ superoxide anion radicals coordinated on surface Zr^{4+} ions.[7,8] The *g*-tensor of this spectrum is g_{xx} = 2.003 g_{yy} = 2.010 g_{zz}= 2.034, whereas the signal intensity corresponds to a concentration of paramagnetic centers of ~2×10^{12} spin g^{-1}, corresponding to about 7×10^9 spin m^{-2}. The g_{zz} value is clearly compatible with a tetravalent adsorption site, so that the assignment to the $O_2^{\bullet-}/Zr^{4+}$ system is straightforward.[7] $O_2^{\bullet-}$ is a very reactive and short-lived species; in solution, it can be detected only by using spin traps,[9] whereas its EPR signal has been observed for solid or amorphous materials subjected to drastic treatments. Specifically, spectra similar to that observed for HSGZ are reported in

Received: July 30, 2015
Accepted: September 23, 2015
Published: September 23, 2015

DOI: 10.1021/acsami.5b06988
ACS Appl. Mater. Interfaces 2015, 7, 21662–21667

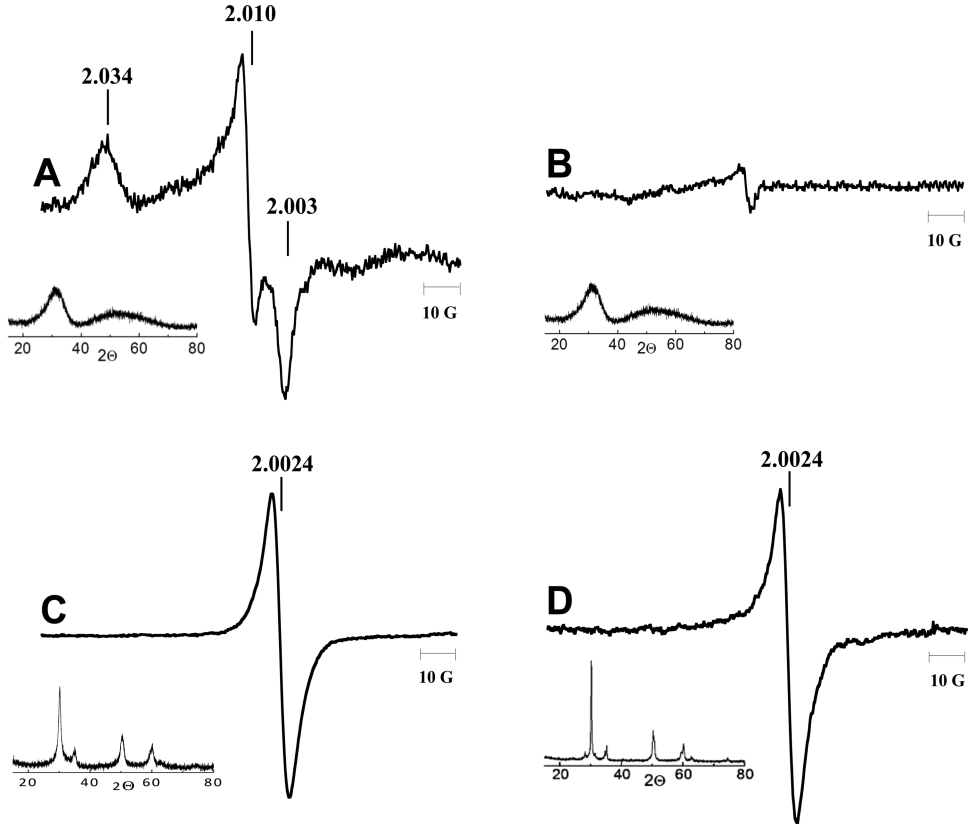

Figure 1. EPR spectra of (A, C) HSGZ and (B, D) SGZ, (A, B) before and (C, D) after annealing at 400 °C for 1 h. The insets show the XRD data for the same materials.

the literature only for crystalline zirconia samples subjected, in order, to (1) activation by a thermal pretreatment in vacuo and (2) contact with oxygen at high temperature or under UV irradiation.[7,8,10,11] In contrast, HSGZ samples analyzed in this work were simply produced at room temperature in the presence of air and kept in the dark for at least 12 h before EPR measurements. Only a very weak singlet was observed for SGZ (ZrO_2 without acac), positioned at g = 2.0024, see Figure 1B, which can be attributed to a few paramagnetic defects due to free electrons localized in oxygen vacancies (F centers).[7,10] Thus, our results show that acac ligands present on the HSGZ surface play a fundamental role in generating and stabilizing the superoxide radical anions. We recorded HSGZ and SGZ EPR spectra also on samples that were heated for 1h at 400 °C, see Figure 1C, D, respectively. Contrary to the initial amorphous samples, in both the annealed ones tetragonal crystalline phase is formed (XRD insets in Figure 1C, D). The annealing of the HSGZ sample produces complete acac ligands removal as ascertained by thermogravimetric analysis (not reported). The spectra of the annealed HSGZ and SGZ show only an intense single peak at g = 2.0024. Quantitatively, for both samples an increased concentration of paramagnetic defects is observed, up to 4×10^{13} spin g^{-1} for annealed HSGZ. However, no evidence of $O_2^{\bullet-}$ formation is observed, thus showing beyond any doubt that acac ligands are necessary to form and stabilize the superoxide anion radicals on the material surface.

The specific role of acac, the mechanism of oxygen adsorption and the origin of the $O_2^{\bullet-}$ species have been investigated by means of ab initio modeling. Several methods have been developed to model amorphous structures.[12,13] A realistic simulation of the bulk structure of amorphous zirconia has been obtained by a "melt-and-quench" ab initio molecular-dynamics approach.[14] However, this approach is computationally demanding, thus hampering studies on surface properties and processes. For this reason we adopted an alternative approach, assuming that the local molecular order of HSGZ/SGZ materials resembles that of the ZrO_2 tetragonal/cubic polymorphs.[15,16] Indeed, both the acac coordination and the adsorption of O_2 to surface Zr species are localized events in the space, so that we have considered the surfaces of our materials as locally ordered for modeling purposes. Rather than a structural representation of HSGZ/SGZ bulk, here we aim at understanding how local specific acac−zirconia interactions affect molecular oxygen adsorption and formation of catalytically active ROS, as observed in experiments.

We performed spin-polarized density functional theory (DFT)-based calculations as implemented in the Vienna Ab initio Simulation Package (VASP)[17] with the Perdew−Burke−Ernzerhof (PBE) gradient-corrected exchange-correlation density functional.[18] To correct for DFT Self-Interaction Error that may lead to unphysical results for defective zirconia, we applied the DFT+U approach[19] with a $U-J$ value of 4 eV for Zr d electrons. To model stoichiometric and defective HSGZ and SGZ surfaces, we used a periodic slab approach and we considered the lowest energy surfaces of cubic zirconia, i.e., (110) and (111) surfaces[20] (further details on computational approach and justification of structural models are reported in the Supporting Information).

We first studied the structural features of acac molecule at ZrO_2(110)/(111) surfaces. In both surfaces, the ligand binds to a single Zr atom with a chelate structure (Figure S1). From analyses of electronic densities, we found that acac forms two

DOI: 10.1021/acsami.5b06988
ACS Appl. Mater. Interfaces 2015, 7, 21662−21667

standard coordination bonds with a single surface Zr ion. Then, we focused on the adsorption of the O_2 molecule on materials surfaces by also taking into account the presence of oxygen vacancies (Vo), which could arise from the local stoichiometric disorder in both HSGZ and SGZ, typical of sol−gel derived materials. Thus, we considered three reactions and the corresponding energies

$$M + O_2 \rightarrow M - O_2^* \qquad \Delta E_1 = E(M - O_2^*) - [E(M) + E(O_2)] \quad (1)$$

$$M \rightarrow M_{Vo} + 1/2O_2 \qquad \Delta E_2 = E(M_{Vo}) + 1/2E(O_2) - E(M) \quad (2)$$

$$M_{Vo} + O_2 \rightarrow M_{Vo} - O_2^* \qquad \Delta E_3 = E(M_{Vo} - O_2^*) - [E(M_{Vo}) + E(O_2)] \quad (3)$$

Where M represents HSGZ and SGZ when considering ZrO_2 surfaces with and without acac, respectively; O_2 is computed in gas phase in its triplet ground state and * denotes the adsorbed oxygen species.

Eq 1 and 3 represent the O_2 adsorption reaction with the corresponding binding energies (ΔE_1 and ΔE_3). Eq 2 represents the formation of an oxygen vacancy defect at the zirconia surface and it is a necessary step for reaction 3 to occur, so that the binding energy for reaction 1, ΔE_1 should be compared to the sum of ΔE_2 and ΔE_3, ΔE_{TOT}. Table 1 lists all the ΔE values.

Table 1. Surface Oxygen-Vacancy Formation Energies and Molecular Oxygen Adsorption Energies for HSGZ and SGZ Model Systems, ΔE (in eV), Computed According To Eqs 1−3

	ZrO_2/acac (HSGZ)		ZrO_2 (SGZ)	
	(110)	(111)	(110)	(111)
ΔE_1	−0.16	0.28	−0.33	−0.02
ΔE_2	2.22	0.34	5.61	6.07
ΔE_3	−3.31	−1.96	−5.08	−5.26
ΔE_{TOT}	−1.09	−1.62	0.53	0.81

Negative ΔE values correspond to convenient binding of the oxygen to the zirconia surface. In the case of the stoichiometric HSGZ and SGZ surfaces the interaction with molecular oxygen is very weak. The adsorbed acac causes steric hindrance for the oxygen binding and the ΔE_1 values are less convenient than for the SGZ. Adsorption becomes even unfavorable for HSGZ (111) surface where the Zr species have already a 7-fold O^{2-} coordination (see the Supporting Information). However, when considering formation of surface lattice defects (i.e., an oxygen vacancy) and O_2 adsorption, the thermodynamic balance is remarkably different between HSGZ and SGZ. In the case of SGZ, the oxygen vacancy formation is very energy demanding (ΔE_2 values above 5.5 eV), the convenient adsorption of molecular oxygen at defect sites is not sufficient to drive the overall energy balance to energetically favorable values ($\Delta E_{TOT} > 0$). In HGSZ, the acac presence lowers significantly the oxygen vacancy formation energies and the subsequent binding of an oxygen molecule provides the necessary energy to obtain a convenient balance ($\Delta E_{TOT} < 0$). In other words, the complexed acac molecule leads to a favorable thermodynamic driving force for a cyclic formation of surface oxygen vacancy and adsorption of molecular oxygen species. It is interesting to note that oxygen is present during the whole experimental procedure of HSGZ preparation, so that initial vacancy formation and oxygen adsorption could happen simultaneously rather than sequentially. However, this does not affect the energy balance. Now we turn our attention to the identification of the oxidation state of these species.

Figure 2 shows the defective HSGZ (110) and (111) model surfaces with the adsorbed oxygen molecule. In the case of

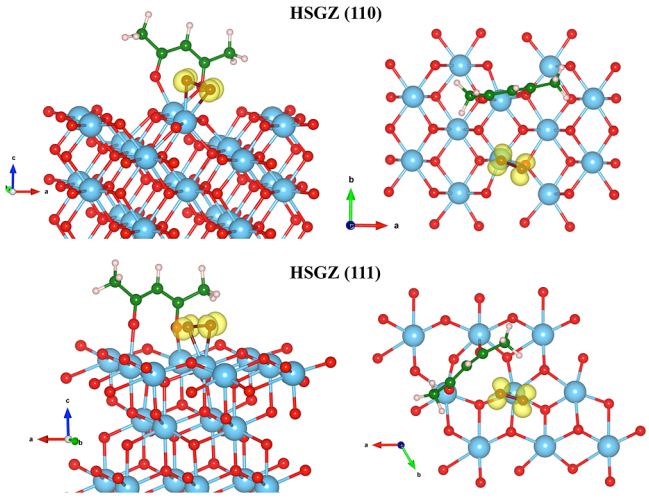

Figure 2. Calculated electron spin density plots of O_2 species adsorbed on defective HGSZ model surfaces. Lateral/Top views at the Left/Right, respectively. Color code: Zr (blue), O (red), adsorbed O_2* (bordeaux), C (green), and H (light pink). Yellow isosurfaces represent the excess of spin up density. Isosurface values are set to 0.01 for clarity.

HSGZ (111), upon formation of the surface oxygen defect the acac molecule changes its coordination from a chelate (Figure S1) to a bidentate configuration. The depicted iso-surfaces represent the electronic spin densities, which are both fully localized onto the oxygen species. To quantify the electron-density rearrangement upon oxygen adsorption we analyzed the electronic spin density in terms of Bader's atom-in-molecule partial charges[21] and atomic magnetic moments. Table 2 lists the O_2 structural and electronic features on pristine and defective HSGZ/SGZ surfaces.

The gas-phase O_2 minimum-energy structure at the DFT-PBE level of theory presents a bond length (d_{O-O}) of 1.22 Å, and the triplet ground state leads to a magnetic moment value of 0.9 μ_B on each O atom. The adsorbed O_2 species present similar characteristics on (110) and (111) surfaces. Upon adsorption on stoichiometric HSGZ surfaces, there is only a slight elongation of the O−O equilibrium distance, a very little charge transfer from the surface to the O_2 molecule (ΔQ_{O2}) and the oxygen atom magnetic moments are consistent with a triplet electronic ground state as in the isolated oxygen molecule. Thus, the acac molecule in pristine HSGZ acts only as a spectator: the oxygen coordinates to a surface Zr ion but keeps its triplet ground state. In contrast, adsorbed oxygen species on HSGZ defective surfaces present an appreciable extent of O−O bond elongation and zirconia-O_2 charge transfer. On both (111) and (110) surfaces, the adsorbed oxygen species retain half of their original magnetic moment, thus proving the formation of superoxide radical ion $O_2^{\bullet-}$

DOI: 10.1021/acsami.5b06988
ACS Appl. Mater. Interfaces 2015, 7, 21662−21667

Table 2. Oxygen Structural and Electronic Parameters of the Oxygen Species Adsorbed on Pristine and Defective HSGZ and SGZ Model Systems: O−O Equilibrium Distance (d_{O-O}), Variation of Electronic Charge on the O_2 Molecule upon Adsorption (ΔQ_{O2}), and Atomic Magnetic Moment on Each Oxygen Atom (μ_O)

			ZrO_2/acac (HSGZ)				ZrO_2 (SGZ)			
			(110)		(111)		(110)		(111)	
stoichiometric	d_{O-O}	(Å)	1.25		1.24		1.27		1.23	
	ΔQ_{O2}	(e^-)	0.17		0.13		0.25		0.03	
	$\lvert\mu_{O1}\rvert$ $\lvert\mu_{O2}\rvert$	(μ_B)	0.7	0.8	0.8	0.8	0.7	0.7	0.8	0.8
reduced (M_{Vo})	d_{O-O}	(Å)	1.35		1.34		1.48		1.48	
	ΔQ_{O2}	(e^-)	1.03		0.93		1.50		1.52	
	$\lvert\mu_{O1}\rvert$ $\lvert\mu_{O2}\rvert$	(μ_B)	0.4	0.4	0.4	0.4	0.0	0.0	0.0	0.0

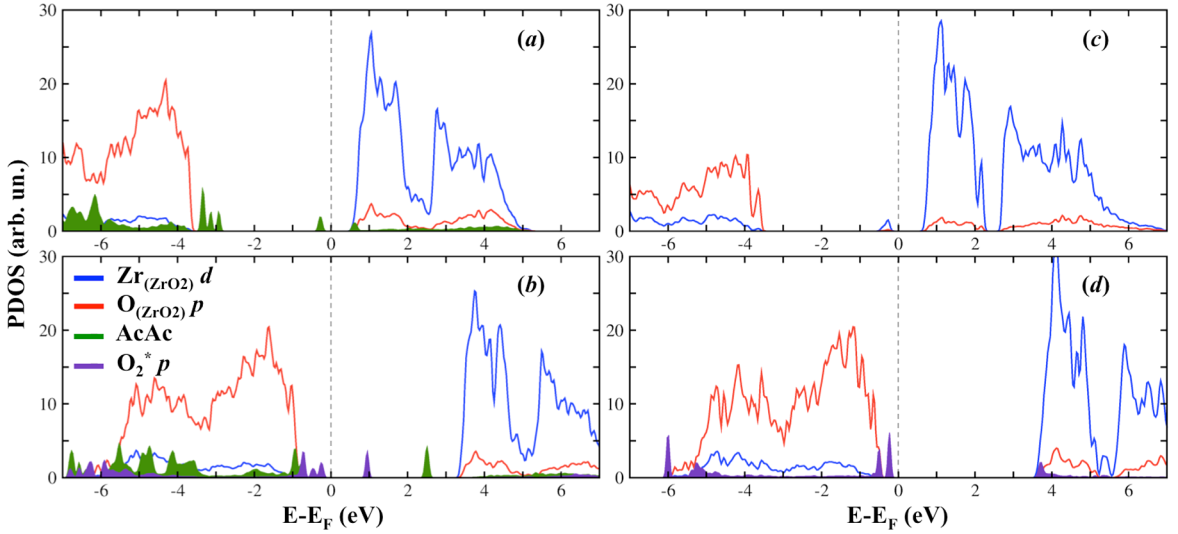

Figure 3. Projected density of states (PDOS) plots computed at the PBE+U level of theory for (a) HSGZ, (b) HSGZ-O_2*, (c) SGZ, and (d) SGZ-O_2* systems. The dashed black line represents the position of the Fermi level. All the plots refer to HSGZ/SGZ (111) model surfaces, the corresponding plots for (110) model surfaces are depicted by Figure S2.

species, which are indeed observed in the HSGZ EPR spectrum. Interestingly, for oxygen species adsorbed onto SGZ surface in the absence of acac, our simulations show a more pronounced elongation of the bond length and annihilation of O atomic magnetic moments is observed, thus depicting a full O_2 reduction to diamagnetic peroxide ion O_2^{2-}. Thus, our simulations confirm the fundamental role played by acac in stabilizing oxygen adsorption and in driving its partial reduction to the radical active species.

The acac role in driving such unexpected behavior can be rationalized by analyzing HSGZ and SGZ electronic structure features before and after O_2 adsorption, as depicted by the Projected Density Of States (PDOS) in Figure 3. Both materials are very likely to have oxygen defects at their solid surfaces. Oxygen vacancy formation leaves two electrons into the system. In the case of HSGZ the excess defect electrons are captured by the acac states that lie within the ZrO_2 bandgap (Figure 3a). The adsorbed oxygen is then only partially reduced to superoxide ion, as proven by the Fermi level crossing the π^* states of the oxygen species (Figure 3b). In case of SGZ, these extra electrons enter the conduction band, made of Zr *d* states, leading to formation of Zr^{3+} ions (Figure 3c). The adsorbed oxygen is then reduced by these high-energy Zr^{3+} species to peroxide ion (Figure 3d).

The electronic structure features arising from PDOS analysis are qualitatively consistent with the results of Diffuse Reflectance UV−vis (DRUV) spectroscopy. The UV−vis absorption spectra of HSGZ and SGZ materials, calculated using the Kubelka−Munk function $F(R\infty)$, are reported in Figure 4. The HSGZ spectrum is characterized by a first peak at about 220 nm and a second one at 300 nm with a shoulder-like queue in the visible region up to 550 nm (Figure 4A). In contrast, SGZ shows an absorption peak in the UV region at wavelengths below about 220 nm. Figure 4 shows that, apart from the presence of the peak at 300 nm, a marked red shift of the absorption edge is seen in the HSGZ material with respect to SGZ one.

A quantitative evaluation of the shift of the absorption edge was obtained by linearization of the plot of $(F(R)h\nu)^{1/2}$ against $h\nu$, as reported in Figure 4B. For the amorphous SGZ material the value 5.4 eV was obtained, consistent with the transition from the valence band (VB) to conduction band (CB), i.e. related to the $O^{2-} \rightarrow Zr^{4+}$ charge transfer transition, in agreement with the band gap value reported in the literature for crystalline zirconia.[22] For HSGZ sample absorption occurs at a much lower $h\nu$ value, 2.6 eV (460 nm). This low value is associated with n $\rightarrow\pi^*$ intraligand electronic transition producing the yellow-brown color of the HSGZ zirconia-acac gel material.[23] The peak at 300 nm is mainly due to $\pi \rightarrow\pi^*$ intraligand electronic transition,[23] a further contribution possibly arising from π(acac) $\rightarrow\pi^*$(acac)/d(Zr) transition that is characterized by a partial ligand-to-metal charge transfer.[24] Overall, the observed spectral features are consistent with the theoretical predictions of acac states lying in between

DOI: 10.1021/acsami.5b06988
ACS Appl. Mater. Interfaces 2015, 7, 21662−21667

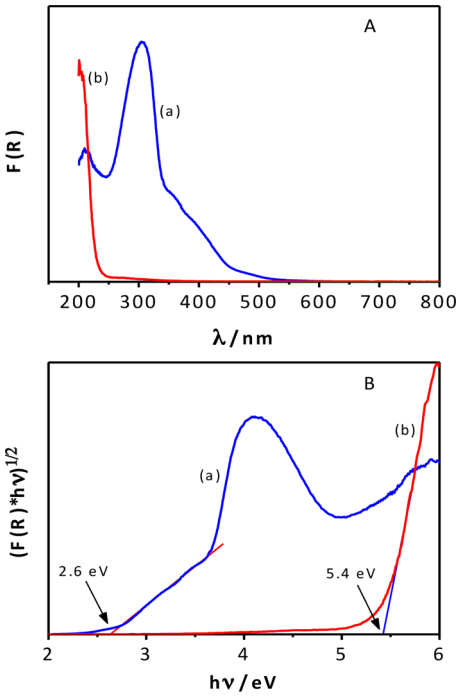

Figure 4. (A) UV–vis absorption spectra and (B) band gap evaluation for (a) HSGZ and (b) SGZ samples.

zirconia valence and conduction bands, see Figure 3 and Figure S2. In this framework, our data would be consistent with a substantial band gap reduction of the HSGZ solid material.

In conclusion, the results presented in this letter demonstrate that the striking HSGZ capability to catalyze oxidative degradation reactions, occurring through a radical mechanism in absence of light and without any thermal pretreatment,[5,6] is due to acac ability in generating and stabilizing the superoxide ion on the hybrid material surfaces. These radical species are still present on the HSGZ surface after a catalytic cycle (see the Supporting Information). EPR measurements and first-principles calculations disclose the origin of such unique feature. Furthermore, the DRUV optical spectra confirm the ab initio electronic structure analyses. Altogether, the experimental evidence and the theoretical results presented in this Letter put on a firm scientific basis the exploitation and further development of HSGZ and related hybrid materials for ROS-based energy and environmental applications.

■ ASSOCIATED CONTENT

Supporting Information

The Supporting Information is available free of charge on the ACS Publications website at DOI: 10.1021/acsami.5b06988.

Minimum energy structure of acac adsorbed on ZrO_2 (110) and (111) pristine surfaces, PDOS plots for the HSGZ/SGZ (110) model surfaces, details of the materials synthesis, EPR and DRUV experimental details, structural model and computational details, and catalytic tests (PDF)

■ AUTHOR INFORMATION

Corresponding Authors

*E-mail: gderrico@unina.it.
*E-mail: mipavone@unina.it.

Funding

A.B.M.G. and M.P. acknowledge funding from the Italian Ministry of Research and University (MIUR) under grants FIRB Futuro in Ricerca (RBFR122HFZ) and PRIN (2012NB3KLK).

Notes

The authors declare no competing financial interest.

■ REFERENCES

(1) Serpone, N.; Emeline, A. V. Semiconductor Photocatalysis — Past, Present, and Future Outlook. *J. Phys. Chem. Lett.* **2012**, *3*, 673–677.

(2) Gionco, C.; Livraghi, S.; Maurelli, S.; Giamello, E.; Tosoni, S.; Di Valentin, C.; Pacchioni, G. Al- and Ga-Doped TiO_2, ZrO_2, and HfO_2: The Nature of O 2p Trapped Holes from a Combined Electron Paramagnetic Resonance (EPR) and Density Functional Theory (DFT) Study. *Chem. Mater.* **2015**, *27*, 3936–3945.

(3) Gionco, C.; Paganini, M. C.; Giamello, E.; Burgess, R.; Di Valentin, C.; Pacchioni, G. Cerium-Doped Zirconium Dioxide, a Visible-Light-Sensitive Photoactive Material of Third Generation. *J. Phys. Chem. Lett.* **2014**, *5*, 447–451.

(4) Janković, I. A.; Šaponjić, Z. V.; Džunuzović, E. S.; Nedeljković, J. M. New Hybrid Properties of TiO_2 Nanoparticles Surface Modified with Catecholate Type Ligands. *Nanoscale Res. Lett.* **2010**, *5*, 81–88.

(5) Sannino, F.; Pirozzi, D.; Vitiello, G.; D'Errico, G.; Aronne, A.; Fanelli, E.; Pernice, P. Oxidative Degradation of Phenanthrene in the Absence of Light Irradiatiion by Hybrid ZrO_2-Acetylacetonate Gel-Derived Catalyst. *Appl. Catal., B* **2014**, *156–157*, 101–107.

(6) Sannino, F.; Pernice, P.; Minieri, L.; Camandona, G. A.; Aronne, A.; Pirozzi, D. Oxidative Degradation of Different Chlorinated Phenoxyalkanoic Acid Herbicides by a Hybrid ZrO2 Gel-Derived Catalyst without Light Irradiation. *ACS Appl. Mater. Interfaces* **2015**, *7*, 256–263.

(7) Anpo, M.; Che, M.; Fubini, B.; Garrone, E.; Giamello, E.; Paganini, M. C. Generation of Superoxide Ions at Oxide Surfaces. *Top. Catal.* **1999**, *8*, 189–198.

(8) Bedilo, A. F.; Plotnikov, M. A.; Mezentseva, N. V.; Volodin, A. M.; Zhidomirov, G. M.; Rybkin, I. M.; Klabunde, K. J. Superoxide Radical Anions on the Surface of Zirconia and Sulfated Zirconia: Formation Mechanisms, Properties and Structure. *Phys. Chem. Chem. Phys.* **2005**, *7*, 3059–3069.

(9) Pieta, P.; Petr, A.; Kutner, W.; Dunsch, L. In Situ ESR Spectroscopic Evidence of the Spin-Trapped Superoxide Radical, $O_2^{\bullet-}$, Electrochemically Generated in DMSO at Room Temperature. *Electrochim. Acta* **2008**, *53*, 3412–3415.

(10) Gionco, C.; Paganini, M.; Giamello, E.; Burgess, R.; Di Valentin, C.; Pacchioni, G. Paramagnetic Defects in Polycrystalline Zirconia: An EPR and DFT Study. *Chem. Mater.* **2013**, *25*, 2243–2253.

(11) Carter, E.; Carley, A. F.; Murphy, D. M. Evidence for O_2^- Radical Stabilization at Surface Oxygen Vacancies on Polycrystalline TiO_2. *J. Phys. Chem. C* **2007**, *111*, 10630–10638.

(12) Houska, J.; Kos, S. Ab Initio Modeling of Complex Amorphous Transition-Metal-Based Ceramics. *J. Phys.: Condens. Matter* **2011**, *23*, 025502/1–025502/7.

(13) Tielens, F.; Gervais, C.; Lambert, J. F.; Mauri, F.; Costa, D. Ab Initio Study of the Hydroxylated Surface of Amorphous Silica: A Representative Model. *Chem. Mater.* **2008**, *20*, 3336–3344.

(14) Zhao, X.; Ceresoli, D.; Vanderbilt, D. Structural, Electronic, and Dielectric Properties of Amorphous ZrO_2 from Ab Initio Molecular Dynamics. *Phys. Rev. B: Condens. Matter Mater. Phys.* **2005**, *71*, 085107/1–085107/10.

(15) Chang, S.; Doong, R. Chemical-Composition-Dependent Metastability of Tetragonal ZrO2 in Sol-Gel-Derived Films under Different Calcination Conditions. *Chem. Mater.* **2005**, *17*, 4837–4844.

(16) Esposito, S.; Turco, M.; Bagnasco, G.; Cammarano, C.; Pernice, P.; Aronne, A. Highly Dispersed Sol–Gel Synthesized Cu–ZrO_2 Materials as Catalysts for Oxidative Steam Reforming of Methanol. *Appl. Catal., A* **2010**, *372*, 48–57.

DOI: 10.1021/acsami.5b06988
ACS Appl. Mater. Interfaces 2015, 7, 21662–21667

(17) Kresse, G.; Furthmueller, J. *VASP the Guide*; University of Vienna: Vienna, Austria, 2003.
(18) Perdew, J. P.; Burke, K.; Ernzerhof, M. Generalized Gradient Approximation Made Simple. *Phys. Rev. Lett.* **1996**, *77*, 3865−3868.
(19) Anisimov, V. I.; Aryasetiawan, F.; Lichtenstein, A. First-Principles Calculations of the Electronic Structure and Spectra of Strongly Correlated Systems: the LDA+U Method. *J. Phys.: Condens. Matter* **1997**, *9*, 767−808.
(20) Christensen, A.; Carter, E. A. First-Principles Study of the Surfaces of Zirconia. *Phys. Rev. B: Condens. Matter Mater. Phys.* **1998**, *58*, 8050−8064.
(21) Bader, R. F. W. *Atoms in Molecules−A Quantum Theory*; Oxford University Press: New York, 1990.
(22) Chang, S.; Doong, R. Interband Transitions in Sol−Gel-Derived ZrO2 Films under Different Calcination Conditions. *Chem. Mater.* **2007**, *19*, 4804−4810.
(23) Petkova, N.; Dlugocz, S.; Gutzov, S. Preparation and Optical Properties of Transparent Zirconia Sol−Gel Materials. *J. Non-Cryst. Solids* **2011**, *357*, 1547−1551.
(24) Georgieva, I.; Danchova, N.; Gutzov, S.; Trendafilova, N. DFT Modeling, UV-Vis and IR Spectroscopic Study of Acetylacetone-Modified Zirconia Sol-Gel Materials. *J. Mol. Model.* **2012**, *18*, 2409−2422.

DOI: 10.1021/acsami.5b06988
ACS Appl. Mater. Interfaces 2015, 7, 21662−21667